This is a repository copy of *Glass beads from Guishan in Iron Age Taiwan: inter-regional bead exchange between Taiwan, Southeast Asia and beyond*.

Article:

Glass beads from Guishan in Iron Age Taiwan: Inter-regional bead exchange between Taiwan, Southeast Asia and beyond

Kuan-Wen Wang [a],[*], Kuang-Ti Li [a], Yoshiyuki Iizuka [b], Yi-Kong Hsieh [c], Caroline Jackson [d]

[a] *Institute of History and Philology, Academia Sinica, No. 130, Section 2, Academia Road, Nangang, Taipei 11529, Taiwan*
[b] *Institute of Earth Sciences, Academia Sinica, No. 128, Section 2, Academia Road, Nangang, Taipei 11529, Taiwan*
[c] *Department of Chemical Engineering, National Tsing Hua University, No. 101, Section 2, Kuang-Fu Road, Hsinchu 30013, Taiwan*
[d] *Department of Archaeology, University of Sheffield, Minalloy House, 10-16 Regent Street, Sheffield S1 3NJ, UK*

ABSTRACT

Archaeological excavations at Guishan in the southern end of Taiwan have recovered more than a hundred glass beads dating to mid-1st millennium CE. This research investigates the exchange of glass beads between Guishan, eastern Taiwan and Southeast Asia, by analysing the styles, chemical composition and microstructure of 64 glass beads from Guishan, using SEM-EDS, EPMA and LA-ICP-MS. The findings suggest that beads with an m-Na-Al glass and v-Na-Ca composition are the most common, supporting evidence for bead exchange between Guishan and Southeast Asia, originated in South Asia and Western Asia. Furthermore, most m-Na-Al glasses were coloured by copper, and different types of copper-based additives may have been used for different colours, indicating the beads may be derived from multiple production centres or workshops via Southeast Asia. Conversely, the glass bead compositions suggest that glass bead exchange between other contemporary sites in Taiwan is less evident at Guishan, except for one type of yellow glass bead containing bone ash which is different. This bone-ash containing yellow glass at Guishan is firstly identified in Iron Age Taiwan as well as around the South China Sea region. Its counterparts are also found from archaeological sites in southeastern and coastal eastern Taiwan, which might indicate small scale glass bead exchange. This evidence together suggests a dynamic glass bead exchange network between Guishan, eastern Taiwan, Southeast Asia and beyond.

1. Background

1.1. Glass bead exchange and beadmaking in Iron Age Taiwan

Glass beads are excellent indicators for exploring exchange activities over time and space, as they are tiny, easy to carry and transport, and are often demanded by various communities as ornaments or prestige goods for certain social or cultural practices. The earliest presence of glass beads in Iron Age Taiwan can be traced back to around 400 BCE in southeastern Taiwan; later in around the 1st quarter of 1st millennium CE, glass beads start to be found in northeastern and southwestern regions, whilst the middle-west region witnesses the use of glass beads since the turn of 2nd millennium (Wang, 2018; Wang and Jackson, forthcoming). Recent research on bead styles, colours and chemical composition has started to show complex intra-, inter- and cross-regional exchange of glass beads within Taiwan and between regions overseas (Wang and Jackson, forthcoming). A general picture is

that the chemical composition of high alumina (m-Na-Al) or plant ash glass (v-Na-Ca) beads shows a mainly drawn technique which suggests a Southeast Asian connection of bead exchange in the 1st millennium, while a transition to a Chinese origin for beads in Taiwan can be seen in the 2nd millennium due to the presence of high lead glass and wound glass beads (Wang, 2018).

In the 1st millennium CE, the Southeast Asian connection further indicates the participation of Taiwan into the cross-regional South China Sea exchange network where there may be circulation of glass objects, raw materials and/or craft knowledge from South Asia and Western Asia. However, the South Asian and Western Asian elements were not influential on the prehistoric material cultures in Taiwan and thus the exchange of glass beads in this period in Taiwan is thought to be mainly with Southeast Asian communities. Within Taiwan, recent analysis by Wang and Jackson (*forthcoming*) started to show a regional distribution of bead colours and styles in the early Iron Age, which is further interpreted as the presence of a regional exchange network along north and

---

east coasts and may be associated with social and cultural factors.

Previous chemical analysis suggests exotic origins of glass beads, in terms of raw materials, in most archaeological sites in Iron Age Taiwan (Wang, 2016; Wang and Jackson, forthcoming). In Taiwan, there is no indication for glassmaking in the Iron Age, but evidence for glass beadmaking has been reported at Jiuxianglan in the southeastern region (Lee, 2005), where the material culture shows a similarity to that from the Guishan site (see below). The glass beadmaking evidence includes a mandrel encircling a glass bead on the tip and a few pieces of glass rods and waste. However, previous investigations have suggested the mismatch of beadmaking methods, chemical composition and microstructure between finished beads and beadmaking waste from the same site (Wang et al., 2019). More importantly, the finished beads indicate a drawn method of manufacture was used, while the waste reveals the wound technique. This has left more questions than answers for the origin and development of glass beadmaking at Jiuxianglan, and Wang and her colleagues suggest that, based on the chronological and spatial context, the practice of wound beadmaking here may be a later presence in the late 1st millennium than the import of drawn glass beads starting in early 1st millennium (Wang et al., 2019). So far, no glass beads from other contemporary sites are found to be locally produced at Jiuxianglan, and currently there is no solid evidence to suggest any glass recycling at Jiuxianglan or other sites in Iron Age Taiwan.

1.2. The Guishan site and its cultural interaction with broad eastern Taiwan

Guishan (or Kueishan, 龜山) is located on a coral reef mound in the Hengchun peninsula, in the southern end of Taiwan (Fig. 1). The name 'Guishan' means 'Turtle Mountain' in Chinese, which describes the turtle shell-like shape of the hill. The earliest reference to Guishan can be traced back to Miyamoto (1931). It was not reported on again until the 1970s when Kaneko (1978) produced a detailed description of the geographic location and the prehistoric remains of the Guishan site. Later in the 1980s further archaeological research was carried out at Guishan, including an initial archaeological survey in the Kenting National Park by Li et al. (1985), followed by other inventory surveys and test excavations in the 1980s and 1990s (Huang et al., 1987; Li, 1995, 1994, 1993; Sung et al., 1992).

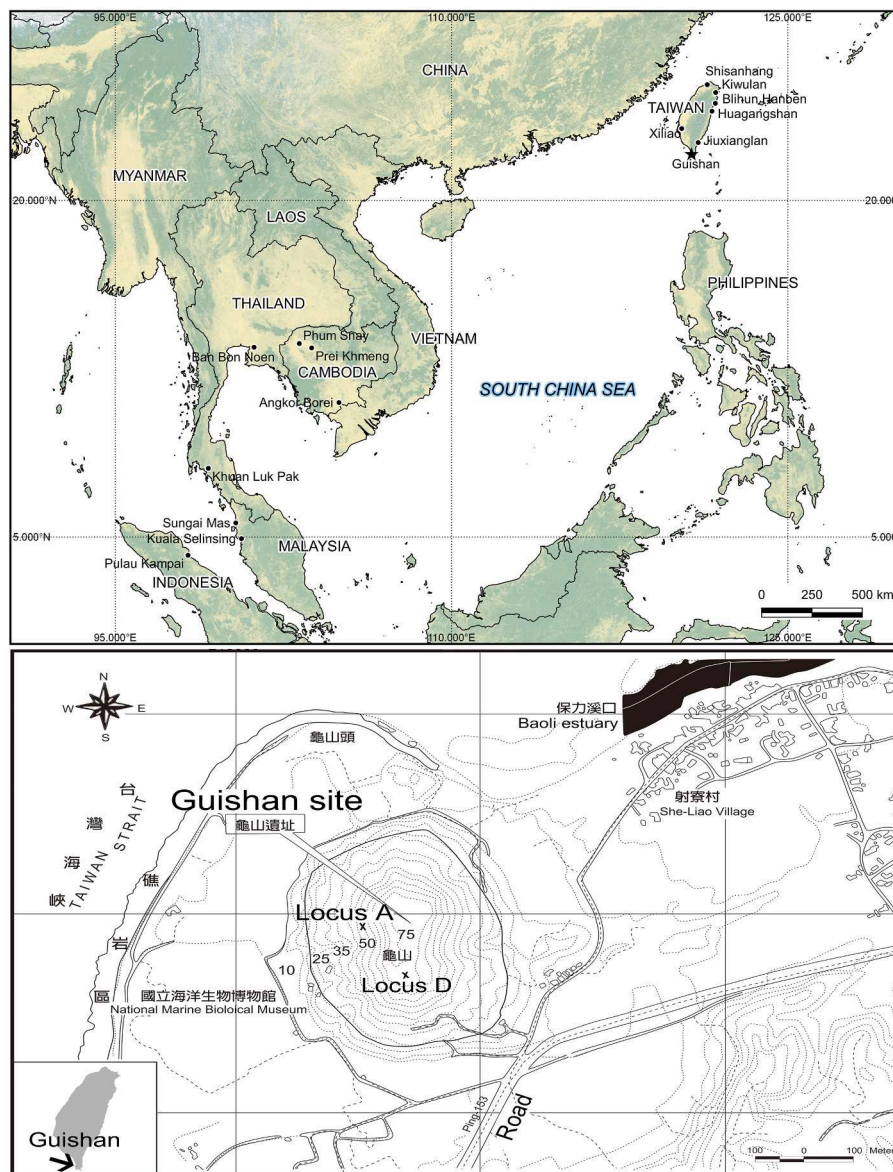These investigations have revealed the presence of Neolithic and Iron

Fig. 1. Map showing the sites mentioned in this article, the location of Guishan, and the excavation units Locus A and Locus D.

Age deposits. The Iron Age deposits have been ^{14}C dated from shells (from an early excavation) which suggest an occupation around the 10th century CE (1082 cal BP) (Chu, p. 110, 1990; Huang et al., 1987; Tsang et al., pp, 1994. 1323-KS-1). In the test excavations of 1993 and 1994, the ^{14}C dates from human bone indicates an earlier chronology of 1470 ± 150 BP and 1525 ± 120 BP (Table 1, and see Li, 1995, p. 67). The calibration using OxCal shows the date to be between 3rd–9th centuries. [14]C dating on shell samples also suggest a similar chronology. It is now generally accepted by Taiwan archaeologists that the Iron Age deposits at Guishan date to mid to late 1st millennium.

The Iron Age finds within this deposit at Guishan have led to the nomenclature of a 'Guishan Culture' (Li et al., 1985). This culture is defined by the presence of unique decorated pottery, glass beads, metal objects, bone objects and slab coffins. The decorated pottery is called 'Guishan style pottery', renowned for a motif of impressed geometric shapes with anthropomorphic and zoomorphic figure, which can be associated with the decorative elements in the material culture of the present-day Paiwan indigenous group in southeastern Taiwan (Li, 2003). This elaborately decorated pottery was initially thought to be found only in the Guishan Culture in the far south Hengchun peninsula of Taiwan. Later archaeological findings in 1990s and 2000s, however, has unearthed this particular type of pottery from several archaeological sites along the southeastern and coastal eastern regions in Taiwan (e.g. Lee and Yeh, 2001; Liu et al., 2002; Tsang and Yeh, 2000; Yeh, 1993).

The presence of the Guishan style pottery in southeastern and eastern Taiwan has triggered discussion about the cultural affinities and exchange activities between the Guishan Culture in the Hengchun peninsula and other cultures, such as Sanhe Culture, in the wider eastern regions, as well as its possible connection to the Philippines to the south of Taiwan. It has been suggested by Kuo (2010) that the complex motif on the Guishan style pottery, together with the presence of glass beads, bronze and iron artefacts, might indicate that overseas migrants moved from northern Luzon in the Philippines to southeastern Taiwan. Within Taiwan, scholars suggest that the presence of Guishan style pottery reflects material exchange along the southern end and eastern coastal areas (Kuo, 2010; Yang et al., 2012; Lee, 2015; Lee and Yeh, 2017). This can be inferred from petrographic research which shows that the raw materials used to produce Guishan style pottery were procured in the southeastern region near Jiuxianglan (Sanhe Culture), suggesting that this type of pottery was not locally produced at Guishan and there were circulation of raw materials or most probably finished objects between the southern end and southeastern regions (Li, 2003; Yang et al., 2012).

'Guishan style pottery' was excavated at Jiuxianglan and other Sanhe Culture sites in southeastern Taiwan (Lee, 2005, 2009, 2015; Liu et al., 2002). Together with similar archaeological assemblages and a burial practice using slab coffins in both the Guishan (sandstone) and Sanhe Cultures (mostly slate), archaeologists have started to suggest cultural affinities between the two cultures, and some believe that the Guishan Culture may be the late phase of Sanhe Culture (e.g. Kuo (2010)). However, Guishan style pottery is also found further north, from sites in eastern coastal Taiwan (e.g. Huagangshan (Chao et al., 2013)) and Blihun Hanben ((Chen, 2017), Fig. 1) where the material assemblages present do not suggest cultural similarities to the Guishan Culture. In

this case, the Guishan style pottery reflects the existence of an exchange network along the southern end and east coast of Taiwan. The networks expressed by the spatial distribution of this distinctive pottery type have thus shown a complex exchange network connecting the southern end and the broader eastern coastal areas. However, this conclusion must remain tentative as previous investigations have mostly focused on pottery analysis and there is a lack of a broader perspective from other categories of artefacts. A comparative study of Southeast Asian materials is also limited, although there was a preliminary assumption of the movement of peoples from northern Luzon in Southeast Asia to this region (Kuo, 2010). It is thus the purpose of this research to explore this potentially complex network using glass beads as a further indicator of exchange patterns within Taiwan and to investigate the possible overseas trade connection with Southeast Asia. Meanwhile, as glass bead-making was reported at the Sanhe Culture site Jiuxianglan, this research also intends to examine the potential association of glass bead and waste assemblages between Guishan, Jiuxianglan and other contemporary sites in Taiwan.

1.3. Glass beads from Guishan

Glass beads were found from test excavations in 1993 and 1994. A total of 123 monochrome glass beads were found, in red, orange, yellow, green, blue, light blue and dark blue colours, all from three burials DB1, DB2 and DB3 in sandstone slab coffins built upon the coral reef, from Locus D, to the south of the site (Fig. 1) (Li, 1994). Both extended supine and prone burials were represented, with multiple skeletons of two, three and four bodies in DB1, DB2 and DB3 respectively. Among the three burials, the majority of glass beads were from DB1 (n = 71) and DB2 (n = 49), where the radiocarbon dating suggests a contemporary chronology of around 3rd to 9th century CE (Table 1). Unfortunately there is no absolute dating for DB3. Other grave goods include glass bracelets, Guishan style pottery, iron blades, bronze bracelets, pig teeth ornaments and perforated human teeth ornaments (Li, 1994, p. 15). Previous research has suggested that the perforated human teeth may be regarded as prestige goods representing the social status of the deceased (Li, 2001).

The physical appearance of these glass beads generally resembles the monochrome glass beads which are widespread throughout southeastern Taiwan and around the South China Sea region (e.g. Francis, 2002 colour plate 9; Hung and Bellwood, p. 242, 2010; Lankton and Dussubieux, p. 69, 2013; Wang et al., 2019). No previous analysis has been carried out on these glass beads to understand their connection to similar counterparts in Iron Age Taiwan as well as in the South China Sea region.

2. Methodology

Sixty-four glass beads were selected for analysis (Table 2). These samples were observed under a stereomicroscope to investigate the styles and beadmaking methods using the 'fabric marks': inconsistencies on the surface of the glass bead which are indicative of the manufacturing method. In drawn beads, parallel striations or bubbles

Table 1
Radiocarbon dates obtained from human bone and shell from Guishan.

Sample No.	Location	Material	Lab Code	[14]C Age (BP)	δ^{13}C (‰)	68.2% Calibrated Age (cal CE/BCE)	95.4% Calibrated Age (cal CE/BCE)
KS DB1[*]	Locus D Burial 1	human bone	GX-20398-A	1470 ± 150	−11.2‰	390-690 CE	240-890 CE
KS DB2[*]	Locus D Burial 2	human bone	GX-20399-A	1525 ± 120	−11.6‰	410-640 CE	240-710 CE (94.6%) 740-770 CE (0.8%)
KSAP1L3[**]	Locus AP1 Layer 3	shell	NTU-3762	2000 ± 30	1.9‰	362-430 CE	315-466 CE
KSAP2L3[**]	Locus AP2 Layer 3	shell	NTU-3769	1910 ± 30	2.0‰	458-535 CE	429-567 CE

[*]: (1) Calibrated using OxCal (INTCAL13). (2) Date based upon Libby half life (5570 years) for [14]C.
[**]: (1) With global marine reservoir correction. (2) Calibration dataset: Stuiver et al. (1998a), Stuiver et al. (1998b), Stuiver and Braziunas (1993).

Table 2
A list of analysed bead samples from Guishan.

Sample number	Burial	Colour	Length (mm)	Diameter (mm)	Shape	Diaphaneity	Stylistic group	Chemical group	Manufacturing method
GS001*	DB2	green	3.31	3.22	short tubular	opaque	GS-G1	m-Na-Al	drawn
GS002	DB2	blue	3.07	2.66	long tubular	opaque	GS-B1	m-Na-Al	drawn
GS003	DB2	yellow	3.18	4.48	short tubular	opaque	GS-Y1	m-Na-Al	drawn
GS004*	DB2	red	6.32	3.28	long tubular	opaque	GS-R1	m-Na-Al	drawn
GS005*	DB2	yellow	2.45	4.65	short tubular	opaque	GS-Y1	m-Na-Al	drawn
GS006	DB2	green	3.06	4.21	oblate	opaque	GS-G1	m-Na-Al	drawn
GS009	DB2	blue	2.46	3.8	oblate	opaque	GS-B1	m-Na-Al	drawn
GS010	DB2	red	3.76	3.81	short tubular	opaque	GS-R1	m-Na-Al	drawn
GS011	DB2	yellow	2.19	4.25	short tubular	opaque	GS-Y1	m-Na-Al	drawn
GS012	DB2	blue	2.87	3.75	short tubular	opaque	GS-B1	m-Na-Al	drawn
GS013	DB2	blue	2.91	4.21	oblate	opaque	GS-B1	m-Na-Al	drawn
GS015_1	DB2	red	4.21	3.09	long tubular	opaque	GS-O1	m-Na-Al	drawn
GS015_2	DB2	orange	4.21	3.09	long tubular	opaque	GS-O1	m-Na-Al	drawn
GS019	DB2	red	6.02	3.9	long tubular	opaque	GS-R1	m-Na-Al	drawn
GS022*	DB2	yellow	3.19	4.89	oblate	opaque	GS-Y1	m-Na-Al	drawn
GS023	DB2	red	7.72	4.89	long tubular	opaque	GS-R1	m-Na-Al	drawn
GS025	DB3	blue	4.06	4.71	short tubular	opaque	GS-B1	m-Na-Al	drawn
GS026	DB3	green	1.74	3.81	oblate	opaque	GS-G1	m-Na-Al	drawn
GS028*	DB1	yellow	3.07	7.21	biconical	opaque	GS-Y2	m-Na-Al	unidentifiable
GS029*	DB1	yellow	2.4	5.91	biconical	opaque	GS-Y2	m-Na-Al	unidentifiable
GS030	DB1	yellow	3.6	5.03	oblate	opaque	GS-Y1	m-Na-Al	drawn
GS031	DB1	green	3.59	4.25	short tubular	opaque	GS-G1	m-Na-Al	drawn
GS033	DB1	blue	2.35	3.94	oblate	opaque	GS-B1	m-Na-Al	drawn
GS034	DB1	green	2.52	2.88	short tubular	opaque	GS-G1	m-Na-Al	drawn
GS037	DB1	green	1.24	2.66	oblate	opaque	GS-G2	m-Na-Al	drawn
GS038	DB1	red	2.92	4.45	short tubular	opaque	GS-R1	m-Na-Al	drawn
GS040	DB1	yellow	3.34	6.22	biconical	opaque	GS-Y2	m-Na-Al	unidentifiable
GS041	DB1	yellow	2.74	6.31	biconical	opaque	GS-Y2	m-Na-Al	unidentifiable
GS043	DB1	blue	3.98	5.17	oblate	opaque	GS-B1	m-Na-Al	drawn
GS044	DB1	green	3.57	4.5	oblate	opaque	GS-G1	m-Na-Al	drawn
GS049	DB1	blue	4.67	3.75	long tubular	opaque	GS-B1	m-Na-Al	drawn
GS050	DB1	red	3.13	4.23	short tubular	opaque	GS-R1	m-Na-Al	drawn
GS052	DB1	green	3.76	3.53	short tubular	opaque	GS-G1	m-Na-Al	drawn
GS053*	DB1	blue	4.96	4.49	long tubular	opaque	GS-B1	m-Na-Al	drawn
GS055	DB1	red	2.38	4.17	oblate	opaque	GS-R1	m-Na-Al	drawn
GS056	DB1	dark blue	6.58	6.3	oblate	opaque	GS-DB1	v-Na-Ca	drawn
GS059*	DB1	dark blue	3.82	6.46	short tubular	opaque	GS-DB1	v-Na-Ca	drawn
GS060	DB1	dark blue	3.82	6.46	oblate	opaque	GS-DB1	v-Na-Ca	drawn
GS064	DB1	yellow	2.41	3.17	oblate	opaque	GS-Y1	m-Na-Al	drawn
GS065	DB1	green	1.26	2.5	oblate	opaque	GS-G2	m-Na-Al	drawn
GS068	DB1	dark blue	4.75	7.03	oblate	opaque	GS-DB1	v-Na-Ca	drawn
GS070	DB2	red	2.51	3.98	oblate	opaque	GS-R1	m-Na-Al	drawn
GS073	DB2	red	2.2	3.74	oblate	opaque	GS-R1	m-Na-Al	drawn
GS074*	DB2	red	3	4.76	oblate	opaque	GS-R1	m-Na-Al	drawn
GS076	DB2	blue	3.19	3.67	short tubular	translucent	GS-B2	v-Na-Ca	wound-like
GS077	DB2	blue	2.71	3.67	short tubular	translucent	GS-B2	v-Na-Ca	wound-like
GS078	DB2	red	2.91	3.83	short tubular	opaque	GS-R1	m-Na-Al	drawn
GS080	DB2	blue	3.14	3.88	short tubular	translucent	GS-B2	v-Na-Ca	wound-like
GS085	DB2	yellow	2.42	3.85	short tubular	opaque	GS-Y1	m-Na-Al	drawn
GS086	DB2	yellow	1.42	3.81	oblate	opaque	GS-Y1	m-Na-Al	drawn
GS087	DB2	yellow	1.48	3.9	short tubular	opaque	GS-Y1	m-Na-Al	drawn
GS098	DB1	dark blue	4.41	6.44	short tubular	opaque	GS-DB1	v-Na-Ca	drawn
GS099	DB1	dark blue	3.76	6.42	short tubular	opaque	GS-DB1	v-Na-Ca	drawn
GS101	DB1	green	1.48	3.01	oblate	opaque	GS-G2	m-Na-Al	drawn
GS102	DB1	red	6.46	3.37	long tubular	opaque	GS-G1	m-Na-Al	drawn
GS103*	DB1	green	2.44	4.18	oblate	opaque	GS-G1	m-Na-Al	drawn
GS104	DB1	green	2.29	4.68	short tubular	opaque	GS-G1	m-Na-Al	drawn
GS108	DB1	green	1.42	2.65	oblate	opaque	GS-G2	m-Na-Al	drawn
GS109	DB1	green	2.64	4.15	short tubular	opaque	GS-R1	m-Na-Al	drawn
GS111	DB1	red	1.78	3.94	oblate	opaque	GS-R1	m-Na-Al	drawn
GS114*	DB1	dark blue	5.72	8.08	oblate	opaque	GS-DB1	v-Na-Ca	drawn
GS116_1	DB1	green	1.17	2.88	oblate	opaque	GS-G2	m-Na-Al	drawn
GS119	DB1	dark blue	7.28	8.03	oblate	opaque	GS-DB2	SLS	unidentifiable
GS120	DB1	blue	2.28	4.31	oblate	opaque	GS-B1	m-Na-Al	drawn
GS122*	DB1	blue	2.82	3.99	oblate	translucent	GS-B1	m-Na-Al	drawn

* Sample analysed by SEM-EDS and EPMA.

appear on the surface, while in wound beads the fabric marks tend to encircle the perforation axis of the bead. In some cases, the manufacturing evidence is too subtle to assess the beadmaking method, so these were recorded as 'unidentifiable'.

Three analytical methods were used to examine the chemical composition and microstructure of the beads: Scanning Electron Microscope analysis equipped with Energy Dispersive X-ray Spectrometer (SEM-EDS), Electron Probe Microanalyser (EPMA) with Wavelength Dispersive X-ray Spectrometers, and Laser Ablation – Inductively Coupled Plasma – Mass Spectrometer (LA-ICP-MS). In the 64 glass bead samples, 13 were analysed by SEM-EDS and EPMA. One glass bead contains two colours (red and orange, GS015), and therefore the

chemical data shows 65 analyses, rather than 64.

SEM-EDS (JEOL JSM-7100F, Oxford EDS) was used to study the microstructure, and EPMA (JEOL JXA-8500F) was used to determine the quantitative chemical composition of micro-areas and crystal phases when it was necessary. The analyses were carried out at the Institute of Earth Sciences, Academia Sinica, Taiwan. SEM-EDS and EPMA required cutting a small piece of the glass, which was then mounted in epoxy resin and cross-sections were polished by alumina compounds and then diamond suspension. The instrument parameters of SEM-EDS were an accelerating voltage of 15 kV, beam current of 0.1nA and working distance of 10 mm. For EPMA, the analytical parameters were an accelerating voltage of 12 kV, beam current of 6nA, a defocused beam diameter of 5 μm for glass matrix and focused beam for identifying crystal phases. Elements analysed by EPMA include Si, Al, Na, K, Mg, Ca, Fe, Pb, Ba, Ti, Mn, Cu, Sn, collected as oxides, and Cl.

Quantitative bulk chemical analyses down to trace elemental level were carried out by LA-ICP-MS. LA-ICP-MS is a micro-invasive technique which ablates only a minute sample of the bead (almost invisible to the naked eye) and was conducted on all 64 beads. This was undertaken at the Department of Biomedical Engineering and Environmental Sciences, National Tsing Hua University, Taiwan. The LA-ICP-MS analysis was carried out using an ICP-MS (Agilent 7500a, USA) connected with a New Wave UP213 laser ablation system. The analytical protocol followed that reported in Dussubieux et al. (2009), with a single spot analysis using beam diameter of 55 μm, a laser energy at around 0.2 mJ, the pulse frequency of 15 Hz and the pre-ablation time of 20 s. Four points were analysed in each sample and averaged. The analytical results are carefully monitored for any chemical variation which may result from crystal relics or inhomogeneous elemental distribution. Any *single* point showing an increase of specific minor or trace elements was removed and some samples were re-analysed to ensure the bulk composition represents the homogeneous glass matrix. The homogeneity is evaluated by relative standard deviation of results from a single sample. ^{29}Si was used as internal standard. The concentrations were calculated using the method proposed in Gratuze (1999), with the assumption of oxide weight percent of major, minor and trace elements equal to 100%. The detection limit was calculated as three times the standard deviation of the blank signals.

Corning Glass standards A, B, C, D and NIST 610, 612 were used as matrix matched standards. Generally, a good precision can be seen in both EPMA and LA-ICP-MS. For major elements, the relative standard deviation (RSD) is lower than 5%, while for minor elements a RSD lower than 20% in EPMA and 8% in LA-ICP-MS (including trace elements except for Sb_2O_5 in Corning C and NIST612). For the accuracy, a relative error of +/- 5% for major elements is reported in both EPMA and LA-ICP-MS, with K_2O frequently measuring lower than the recommended value. For minor elements in weight percent level, the relative error of +/- 60% is reported, except for MnO and Sb_2O_5 in Corning C.

The detection level of MnO was low in EPMA (0.03 wt%) and LA-ICP-MS (0.001 wt%). Here, the LA-ICP-MS result corresponds to the value of MnO reported in Dussubieux et al. (2009) and Wagner et al. (2012) and so is considered reliable. The low measured value of Sb_2O_5 analysed by LA-ICP-MS is also reported in Dussubieux et al. (2009) and Wagner et al. (2012), although the measured Sb_2O_5 in this research (0.0006 wt%) is higher than that in Dussubieux et al. (2009) and Wagner et al. (2012) (~0.0001 wt%). For minor and trace elements recorded at ppm, the relative error of +/- 5% is found for most elements of hundreds ppm, while a greater relative error of ±15% is found for most elements below 100 ppm.

Accuracy of the inter-instrument evaluation between EPMA and LA-ICP-MS in this research is shown in Fig. 2, comparing the EPMA and LA-ICP-MS values for Corning glass standards A, B, C and D. There is generally a good consistency for most elements. However, Na_2O and PbO at minor elemental levels are often underestimated by LA-ICP-MS, while there is an underestimation of SnO_2 in EPMA. The inter-instrumental differences are treated with caution when comparing these elements in this research.
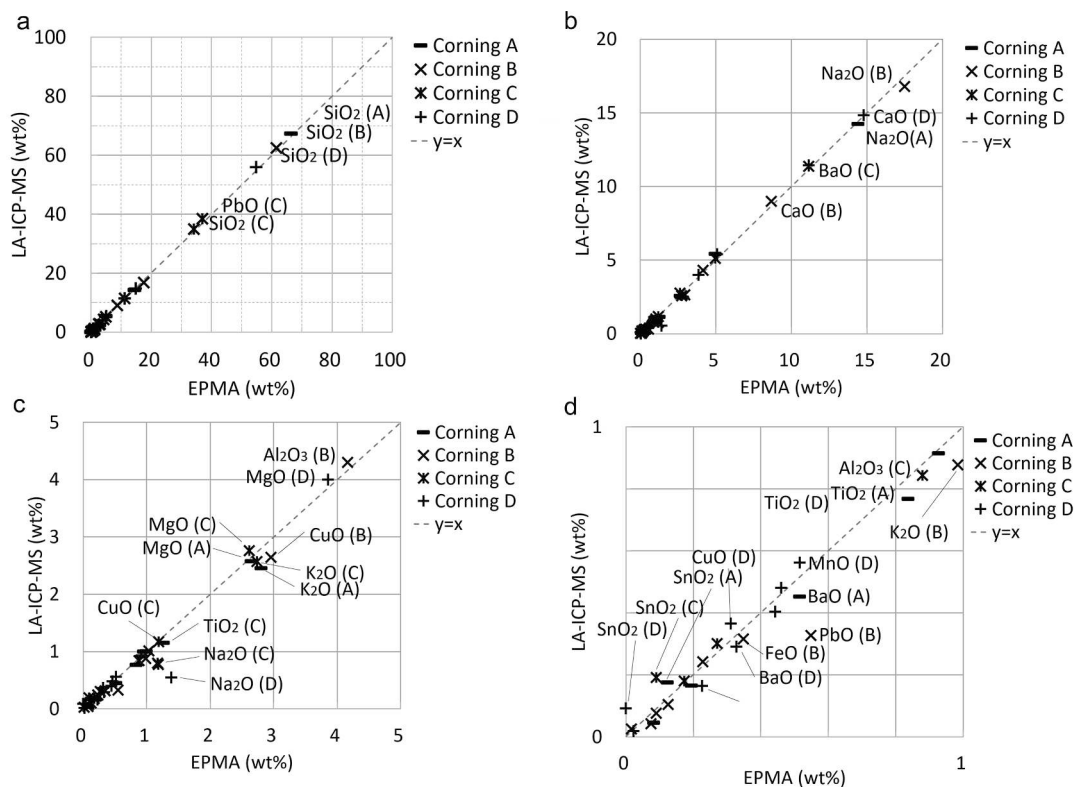

Fig. 2. Inter-instrumental comparison between EPMA and LA-ICP-MS in this research, with chemical concentration of analysed elements in the standards of (a) up to 90 wt%, (b) up to 20 wt%, (c) up to 5 wt% and (d) below 1 wt%

3. Results

3.1. Bead shapes, styles and beadmaking methods

The glass beads are grouped into 10 styles based on their colours, shapes and beadmaking methods (Fig. 3). For an easier description of each stylistic group, the group is prefixed by the site name (GS) and then colour (R = red, O = orange, Y = yellow, G = green, B = blue, DB = dark blue), followed by the proposed beadmaking method (1 = drawn, 2 = wound or other methods).

Glass beads from Guishan show a balanced distribution of red (n = 27), yellow (n = 32), green (n = 27) and blue (n = 22) colours. There are 14 dark blue glass beads and only 1 orange-red bead (orange surface, red body) at Guishan. A great number of beads are made by the drawn method (n = 113), where striations parallel to the perforation can be clearly seen in most cases. These drawn beads are all opaque, of a tubular or oblate shape, with a red, orange, green, blue or dark blue colour. The 4 beads in the GS-B2 group, with a translucent blue colour and a tubular shape, are likely to be wound, based on the coiled marks on bead surface, although the slightly corroded surface may hinder identification of the manufacturing evidence. The beadmaking methods are hard to evaluate on 6 samples, including the 5 yellow beads within GS-Y2 group and 1 dark blue bead of the GS-DB2 group. For the GS-Y2 group, all beads are biconical (Fig. 3). It is apparent that bead shaping using specific tools was carried out on these biconical beads and so the manufacturing evidence is likely to be erased during the shaping process. The only sample in the GS-DB2 group is a dark blue bead with a barrel shape. No obvious manufacturing marks are noted on the bead surface or perforation side, which discriminate this sample from the GS-DB1 group where distinct longitudinal striae, suggesting the drawn method was used, are observed on all samples of a tubular or oblate shape.

Glass beads from Burial 1 comprise more diversity of bead styles (Table 3). All dark blue glass beads (GS-DB1 and GS-DB2) were from Burial 1. The GS-Y2 yellow beads and GS-G2 green beads are only seen in Burial 1 as well. In comparison to GS-Y1, GS-Y2 beads all have a biconical shape and are more opaque than GS-Y1. The GS-G2 beads are smaller and have a darker green colour than GS-G1. The only orange-red glass bead is from Burial 2. In terms of Burial 3, there are smaller quantities of glass beads and only green (GS-G1) and blue (GS-B1) beads are found here. It was suggested that the glass beads may be strung with perforated human teeth in Guishan burials, which display the high social status of the deceased (Li, 2001). The distribution of glass bead styles

and quantities in the three multiple burials may indicate degrees of social variation, although the poor preservation of the skeletons makes it hard to obtain comprehensive bio-archaeological information for further discussion.

3.2. Chemical composition and microstructure

Three chemical groups are identified, namely mineral soda alumina glass (m-Na-Al glass, n = 54), vegetal soda lime glass (v-Na-Ca glass or plant ash glass, n = 10) and soda lime silica glass (SLS, n = 1) (Fig. 4, and see Supplementary Material for full chemical composition). The orange-red glass bead, GS015, was analysed on the outer orange and inner red glasses respectively, so there are two datasets for GS015. Of the 64 beads, 2 red, 2 yellow, 3 green and 2 blue beads were analysed by SEM-EDS to understand their microstructure, which together with the minor and trace elements, reveals more about the raw materials used to produce each colourant.

3.2.1. m-Na-Al Glass

The m-Na-Al glass composition is the largest group here, which contains Na_2O between 10 and 20 wt%, $Al_2O_3 > 10$ wt% and CaO around 2.5 wt%. The MgO is generally <1 wt%, which indicates the use of mineral soda flux. However, greater MgO between 1 and 2.5 wt% is seen in a few red samples, and this may be an effect from the raw materials related to colourant (see below). Most m-Na-Al glass beads from Guishan are drawn glass beads. The colours include opaque red, orange-red, yellow, green and blue. They have an oblate or tubular shape. The high Ba (0.02–0.2 wt%) and low U (generally below 20 ppm) contents suggest that these m-Na-Al glasses belong to the m-Na-Al sub-type 1, as identified by Dussubieux et al. (2010).

Copper-based colourants are predominant in most m-Na-Al glass, including red, orange, blue and green colours. The red and orange glasses are both coloured by cuprous oxide or metallic copper, with the CuO content below 2 wt% in red glass and ~7 wt% in the orange glass. In contrast, the blue glass is coloured by cupric copper, containing CuO below 2 wt%. Increasing amounts of MgO and FeO are seen in the orange and some red glass samples (Fig. 5), which possibly suggests the intentionally introduction of FeO into the red and orange glass to enhance the reduction of cuprous copper, the MgO may be brought in with FeO (Dussubieux et al., 2010). However, unlike the m-Na-Al sub-type 1 glass reported by Dussubieux et al. (2010), a few red samples do not show this correlation, and the enrichment of CaO observed by Dussubieux and her colleagues (2010) is not seen in Guishan samples. In the green glass,
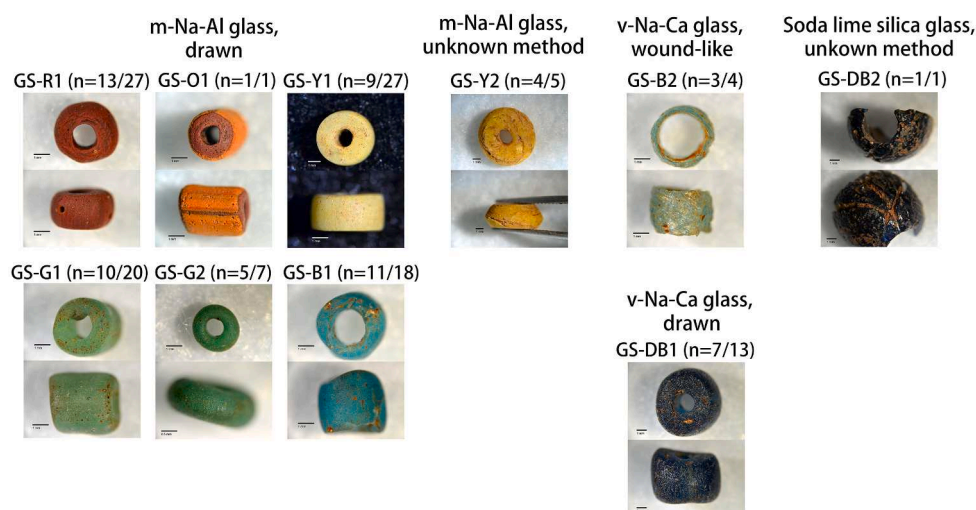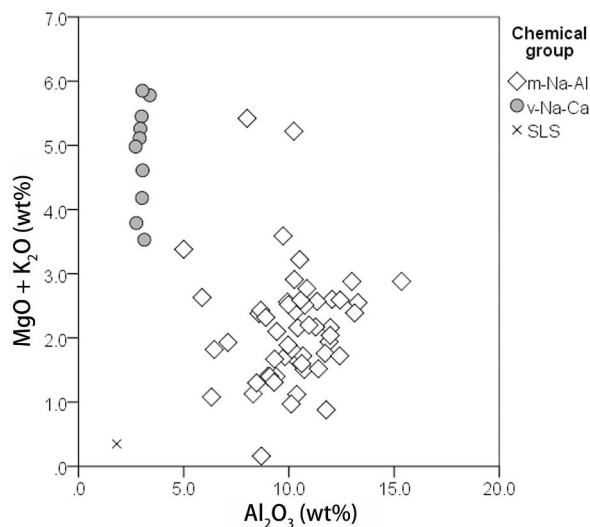

Fig. 3. Different groups of glass beads from Guishan, groups based on colour, shape, chemical composition and beadmaking methods. Within the parentheses, the former number implies the sample numbers analysed by LA-ICP-MS, and the latter number is the total numbers found in that bead style.

Table 3

The distribution of bead colours and styles in the three burials at Guishan.

| Burials	GS-R1	GS-O1	GS-Y1	GS-Y2	GS-G1	GS-G2	GS-B1	GS-B2	GS-DB1	GS-DB2	Total
Burial 1 (DB1)	9		8	5	14	7	13	1	13	1	71
Burial 2 (DB2)	18	1	19		4		4	3			49
Burial 3 (DB3)					2		1				3
Total	**27**	**1**	**27**	**5**	**20**	**7**	**18**	**4**	**13**	**1**	**123**

Fig. 4. The bivariate plot of Al_2O_3 and $MgO + K_2O$, showing the chemical groups of glass beads from Guishan

both cupric copper and lead tin oxide are the colourants, with CuO around 2 wt%, PbO below 3 wt% and SnO_2 no more than 0.5 wt%.

Some different concentrations of minor or trace elements associated with copper are observed in red, orange and blue glass, which may suggest varied types or recipes of copper-containing ingredients were used. A greater concentration of As and Ni is detected in the orange glass (As ~ 1170 ppm, Ni ~ 1300 ppm) than in the red and blue glasses (As < 100 ppm, Ni < 300 ppm). The PbO and SnO_2 concentration increases linearly with CuO in the blue glass (Fig. 6 (a) and (b)), which suggests that the PbO and SnO_2 may be impurities introduced with copper. In the red glass, although elevated levels of SnO_2 and PbO are seen in some samples, unlike the blue glass, there is no linear relationship. It is also noteworthy that, in the orange-red glass bead GS015, the copper-related elements, such as As, Ni, Ag and Sb, do not exhibit any consistent pattern, which indicates that the orange and red glass in this sample are separate glass pieces rather than a single glass in which the red and orange colours are achieved by the control of the redox condition of copper oxide. This argument can be further supported by the joining mark of the orange glass layer shown on the bead lateral surface and cross-section of the perforation (Fig. 3), which reinforces the observation that the orange glass intentionally covers the red glass.

It must be mentioned that, although the presence of various types of copper-based phases is seen in different colours of glass (see below), the analysis of the bulk composition here carefully removes any single analytical point in which the elevated level of minor and trace elements may result from the detection of uneven distribution of separated phases, crystals or particulates. The microstructure of the red and blue glass presented below also reveals a homogenous matrix or even distribution of particles, and thus the influence of heterogeneous phases or crystals on the bulk composition of red, orange and blue glass is thought to be reduced to a minimum here. More discussion on the glass homogeneity obtained using the LA-ICP-MS method can be found in Dussubieux et al. (2009).

Using SEM-EDS the differences related to the copper-containing
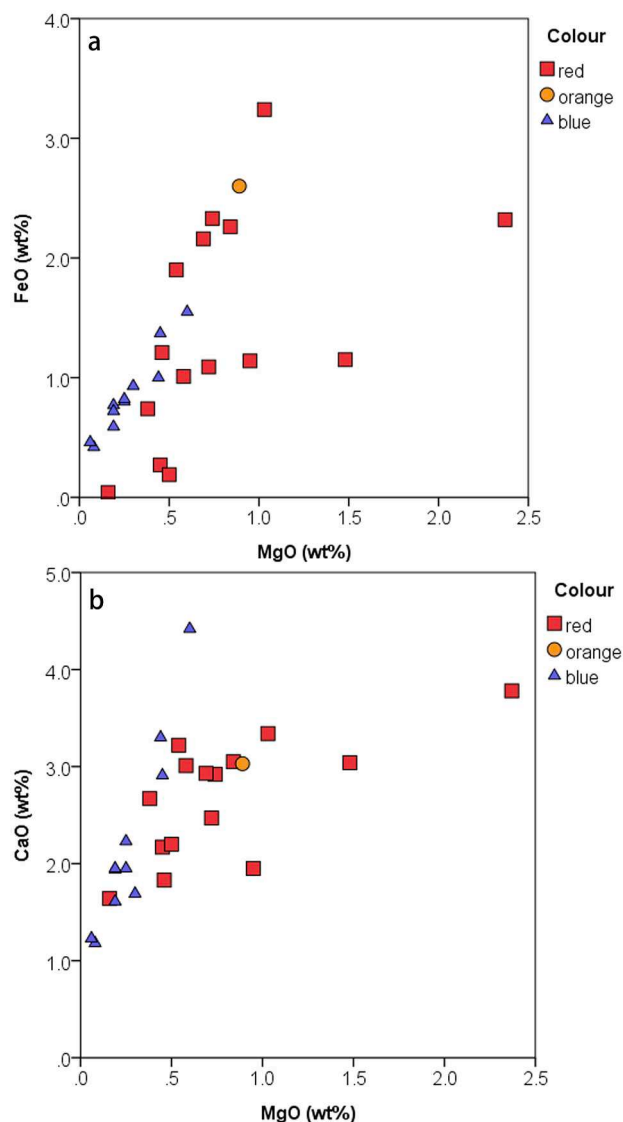
Fig. 5. Bivariate plot of (a) MgO-FeO, and (b) MgO-CaO, showing enrichment of MgO and FeO, but not CaO, in red and orange glass and the linear correlation in a proportion of the red and blue glasses. (For interpretation of the references to colour in this figure legend, the reader is referred to the web version of this article.)

colourant are evident in the red and blue glass. In red glass, minute copper-bearing precipitations are evenly distributed through the matrix, which may contribute to the opacity of the red glass (Fig. 7a). Most precipitations, probably of metallic copper, are much smaller than 1 μm (too small to be confirmed by SEM-EDS), while some particles have a size of around 1–2 μm and contain sulphur (around 7 at%). Large copper-containing droplets of copper sulphide or copper oxide were occasionally observed, with a diameter of around 10 μm which often have smaller voids attached to the particle edge (Fig. 7b and c). It is likely that some of these large droplets are un-melted raw materials of
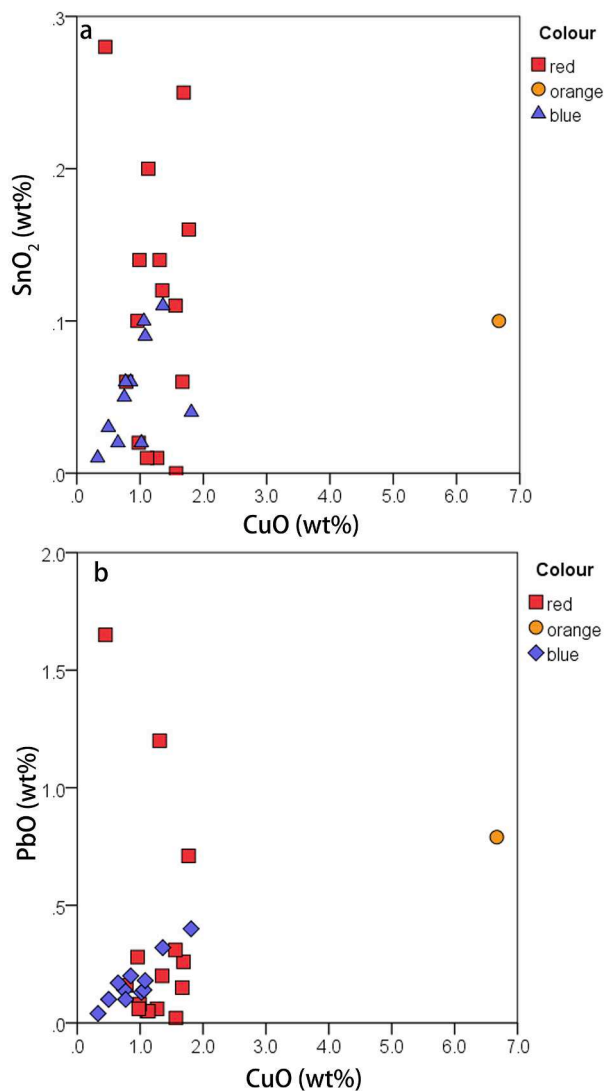
Fig. 6. The bivariate plot of (a) CuO-SnO₂, and (b) CuO-PbO in the red, orange and blue glass from Guishan, showing the linear correlation in the blue glass but not in the red glass. (For interpretation of the references to colour in this figure legend, the reader is referred to the web version of this article.)

the copper colourants, as the inner part of droplet shows slight decomposition, and voids of a similar size and shape were sometimes found over the matrix (Fig. 7a). In comparison to the red glass, the matrix of the blue glass is relatively homogenous, without any visible copper-rich particles (Fig. 7d). The opacity of the blue glass may be mostly attributed to the unmelted minerals such as sodium aluminosilicate and zircon, which are typical in the m-Na-Al glass found in Iron Age Taiwan (Wang, 2016). One possible reason for the presence of sulphur-containing copper in red glass, but not in blue glass, may be the use of different types of copper-containing raw materials, although the redox conditions and temperature of molten glass may also influence the formation, and solubility, of sulphides in the glass melt (Beerkens, 1999; Lopes and Shelby, p. 41, 2007).

The colourant in yellow glass is lead tin oxide. This glass has variable PbO at 2–13 wt% and $SnO_2 < 2$ wt% (bulk composition). The matrix of yellow glass shows an inhomogeneous distribution of PbO, which varies from 13 wt% to 34 wt%, with frequent crystals of lead tin oxide containing 5–6 at% of silicon (Fig. 7e). The atomic ratio of Pb to (Sn + Si) is close to 1:1, suggesting that the lead tin oxide is $Pb(Sn,Si)O_3$. In the yellow glass, newly-formed rectangular nepheline crystals ($NaAlSiO_4$)

and hexagonal sulphur-rich sodalite crystals ($Na_8Al_6Si_6O_{24}(Cl_2,S)$) (formed during glassmaking or glass colouring) are sometimes clustered with lead tin oxide (Fig. 7f and g). In the m-Na-Al glass, un-melted soda-rich feldspars such as plagioclase ($(Na,Ca)(Si,Al)_4O_8$) and albite ($NaAlSi_3O_8$), which may be associated with the glass sand or flux, are frequently seen by SEM-EDS. The nepheline or sodalite near the lead tin oxide aggregations may result from the interaction between the feldspars (and possibly sulphur-bearing ingredients in the case of sodalite) in the glass sand and the lead- and/or tin-containing compounds.

Two yellow biconical beads, GS028 and GS029, of the GS-Y2 stylistic group show the presence of bone ash by SEM-EDS (Fig. 8a–d), with CaO 10–31 wt%, P_2O_5 21–33 wt%, PbO 13–25 wt% and Al_2O_3 and SiO_2 vary from a negligible amount to 30 wt% respectively. Small crystals of lead tin oxide were often found near the bone ash particles, and sometimes inside the bone ash, which suggests that the bone ash may be related to the colouring process (Fig. 8a). The yellow colour of these two samples are more vibrant and opaque than other samples. Together with detectable Al_2O_3 and SiO_2 contents, the bone ash mixture probably contains some aluminosilicate, and was intentionally added to produce the yellow colour, or to increase the glass opacity.

In GS028 and GS029, nepheline and sodalite are also found, both associated with lead tin oxide. In most cases, the shape of lead tin oxide is equant (Fig. 8e), as those typically seen in other yellow glass samples. A sub-angular aggregation of needle-like lead tin oxide ($Pb(Sn,Si)O_3$ containing 2–6 at% of silicon), clustered with nepheline, is seen in GS028 (Fig. 8f). The aggregation is likely to be a partially reacted lump of lead–tin calx which did not fully decompose into the cubic form of $Pb(Sn,Si)O_3$.

In terms of the green glass, the principal difference between GS-G1 and GS-G2 group is the Ba and Sr contents. Samples from GS-G2 exhibit lower Ba (<0.06 wt%) and Sr (<350 ppm) than those in GS-G1 group. A consistent Ba/Sr ratio closes to 1.6 is seen in GS-G2 samples but not in GS-G1 samples, which varies between 1.2 and 4.2. The microstructure of the green glass is similar to the yellow glass. The matrix also shows uneven distributions of PbO from a negligible amount to as high as 16 wt%. The main difference between the green and yellow glass matrix is the presence of around 2 wt% CuO in the matrix of green glass, suggesting that the colouring of green glass is a mixed effect of yellow and blue glass. A cluster of lead tin oxide and sodalite crystals can be observed in the green glass (Fig. 7h), although here the sodalite is chlorine-rich rather than sulphur-rich. The formation mechanism of sodalite seen in green glass may be similar to that in the yellow glass.

3.2.2. V-Na-Ca Glass

V-Na-Ca glass is the second largest chemical group found in the Guishan beads. Both drawn and wound methods are observed in this chemical group, and these beads are either of a transparent blue (GS-B2) or opaque dark blue colour (GS-DB1). For v-Na-Ca glass, the concentration of Na_2O is between 15 and 20 wt%. CaO is generally between 4 and 8 wt%, which is typical of soda plant ash glass. MgO is around 3 wt%, indicating the use of plant ash as raw material of flux (Na_2O).

The relationship of MgO to K_2O is commonly used to discuss the possible variation of plant ash recipe in glassmaking (e.g. Mirti 2008; 2009; Henderson 2004). It can be seen in Fig. 9 (a) that, while comparing to other v-Na-Ca glass within Taiwan, the Guishan samples exhibit lower MgO and K_2O, with some overlap with samples from the Shisanhang site in northern Taiwan. Clearly different groupings can be found between Guishan and Kiwulan (northeastern Taiwan). The K_2O in the Guishan sample (GS099) routinely measured under the detection limit, and thus this sample is tentatively regarded as an outlier here. Further comparison to previous research on Southeast Asian samples reveals a similar pattern as seen in Taiwan. Fig. 9 (b) shows that most Southeast Asian samples have greater MgO and K_2O than those from Guishan and are grouped with other Iron Age samples from Taiwan. Exceptions can be seen in Cambodia and a few Malaysian cases, which generally fall into the range of Guishan with slightly lower level of MgO.
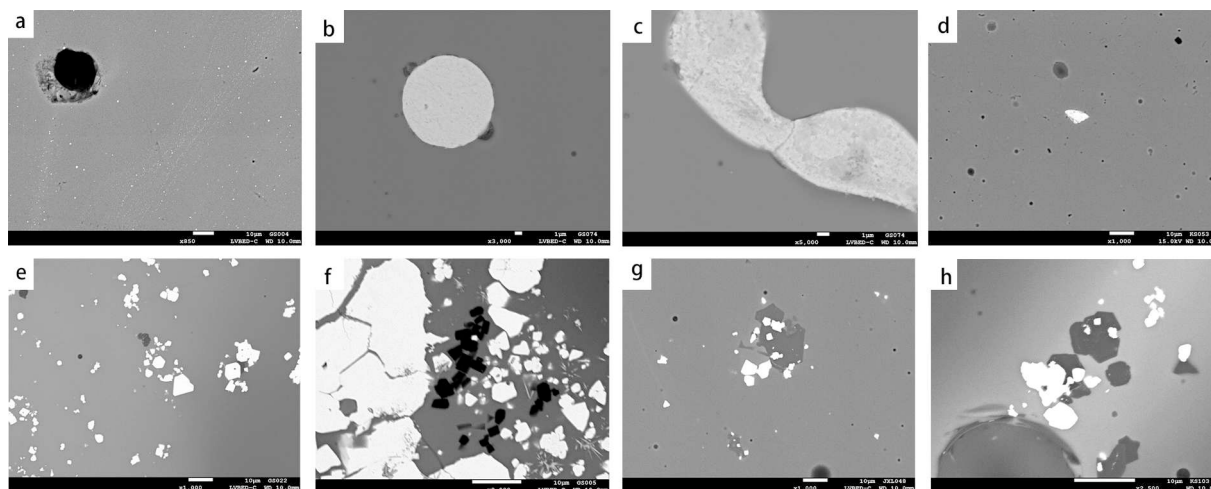
Fig. 7. The SEM BSE (backscattered electron) micrographs of glass samples from Guishan. (a) The matrix of red glass, showing the distribution of minute copper-based precipitations (GS004); (b) The copper sulphide droplet in red glass (Cu 68 at%, S 32 at% GS074); (c) The copper oxide droplet in red glass (Cu 50 at%, O 50 at %, GS074); (d) The homogeneous matrix of blue glass (GS053); (e) the matrix of yellow glass, showing the inhomogeneous distribution of PbO (GS022); (f) the cluster of nepheline (dark crystal) with lead tin oxide (bright crystal) in the yellow glass (GS005); (g) the cluster of sodalite (dark grey crystal) and lead tin oxide (bright crystal) in the yellow glass (GS005); (h) The inhomogenous matrix and the cluster of sodalite and lead tin oxide in the green glass (GS103). (scale bar for a, d, e, f, g, h: 10 μm; scale bar for b, c: 1 μm).
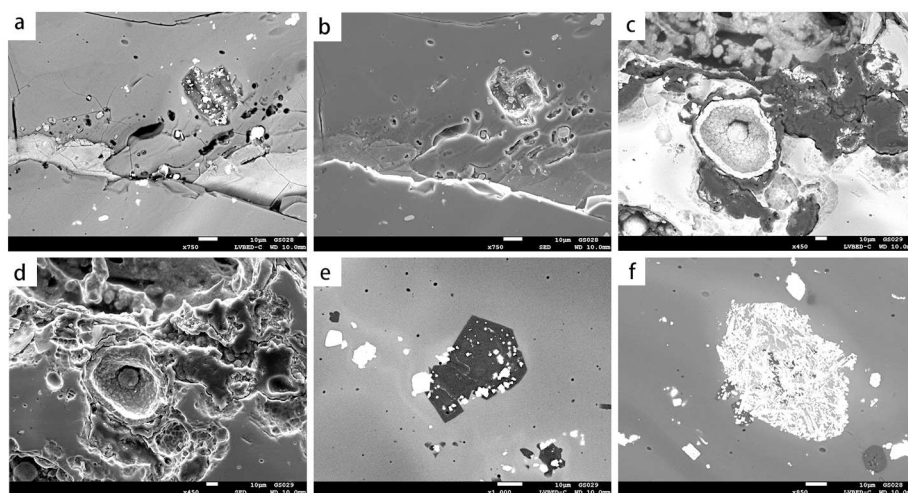

Fig. 8. The SEM micrographs of yellow glass containing bone-ash mixture from Guishan. (a) the BSE image showing bone ash mixture (light grey) and the lead tin oxide crystals (bright) (GS028); (b) the secondary electron image (SEI) of a; (c) the BSE image showing bone ash (round in the middle) embedded in Pb-rich matrix (GS029); (d) the SEI image of c; (e) the cluster of nepheline (dark crystal) and lead tin oxide (bright crystal) in this type of glass (GS028); (f) the sub-angular lump of needle-like crystals of lead tin oxide, clustered with small crystals nepheline (GS028). (scale bar: 10 μm).

V-Na-Ca glass from around the South China Sea is much less studied than m-Na-Al glass. It was suggested by Dussubieux and Allen (2014) and Dussubieux (2014) that three primary sub-groups of v-Na-Ca glass exist in this region. This assertion is based on the contents of Na_2O, Al_2O_3, CaO, Ti and Zr in glass samples from peninsular Malaysia and North Sumatra dated to 9th-13th century CE. When comparing these defined groups to the Guishan samples, the v-Na-Ca glass from Guishan does not fit well with any of these sub-groups. This may be because the chronology of the defined sub-groups in Southeast Asia is later in date than the Guishan samples. Taken together with the MgO and K_2O variation seen above, this possibly suggests a different origin of v-Na-Ca glass at Guishan and other Southeast Asian cases with an early date (more discussion below). The v-Na-Ca glass here also suggests that the chronological range of v-Na-Ca glass is extended for glasses analysed from Southeast Asia and/or more elements need to be considered for future studies of the v-Na-Ca sub-types in this broad geographical area.

The light blue glass is coloured by cupric copper (~0.4 wt% CuO), while the dark blue glass is coloured by cobalt (230–400 ppm). The dark blue samples also show increasing amounts of MnO between 0.1 and 0.3 wt%, but no specific correlation with other elements was found.

It is noted that GS-B2 and GS-DB1 samples exhibit different Zr-Ce relationships. Generally, a linear correlation is seen in the GS-DB1 group as well as most v-Na-Ca glass beads from Taiwan, except for the glass waste from Jiuxianglan site in southeastern Taiwan (Fig. 10). A similar trend is also seen in most samples from Cambodia, Malaysia and Indonesia in Southeast Asia (discussed below), although some Malaysian glasses have greater Zr contents. In addition, GS-B2 samples also have lower CaO and Sr contents than GS-DB1 samples. Zr and Ce are likely to be introduced with sand, and Sr may be added with lime-bearing materials. The varied correlation of Zr-Ce and CaO-Sr seen in GS-B2 and GS-DB1 beads possibly indicate the use of different sources of silica and lime ingredients.

3.2.3. Soda lime silica glass

Only 1 soda lime silica glass was found at Guishan, containing SiO_2 70 wt%, Na_2O 22 wt%, CaO 5 wt% and MgO below 1 wt%. The low MgO content suggests the use of mineral soda flux in glassmaking. This is a dark blue glass bead (GS-DB2), with a different barrel shape from other tubular dark blue glass beads (GS-DB1) from the same site. Soda lime silica glass is rarely reported in Southeast Asia and Taiwan in this period.
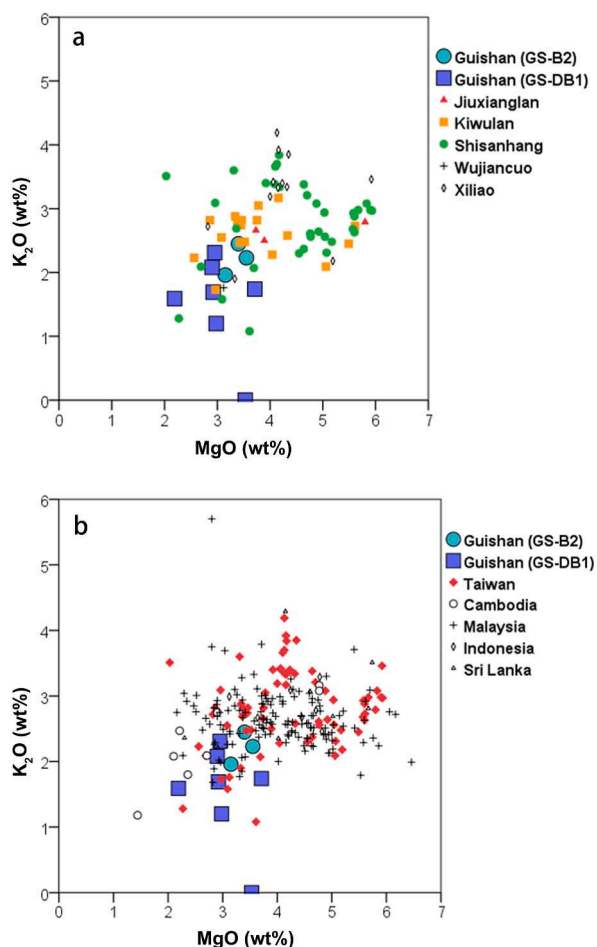
Fig. 9. The bivariate plot of MgO-K$_2$O, showing variation of MgO and K$_2$O in v-Na-Ca glass between Guishan and sites in (a) Taiwan and (b) Southeast Asia. Comparative data of other sites are derived from Carter (2013), Dussubieux (2001), Dussubieux and Allen (2014), Dussubieux and Soedewo (2018) and Wang (2016).
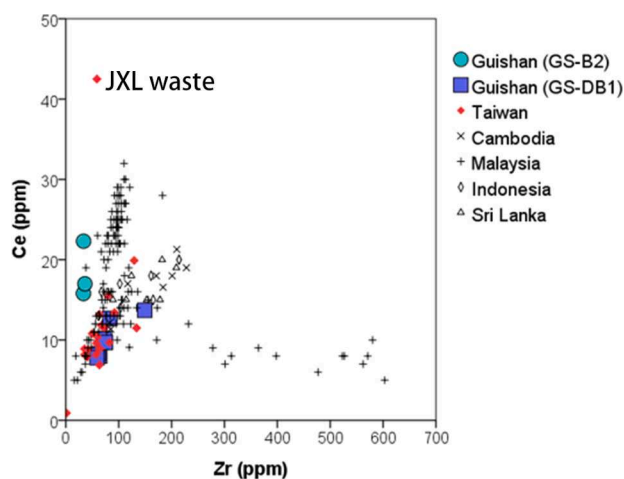

Fig. 10. The bivariate plot of Zr-Ce in the v-Na-Ca glass. The varied linear relationship is seen in GS-B2 and GS-DB1 samples. Similar Zr-Ce correlation can be seen in some samples from other sites in Iron Age Taiwan and Southeast Asia, while a few Malaysian samples show particular high Zr.

Due to the lack of enough comparable data, its origin remains unclear. As yet, a similar chemical composition is reported in only one greenish blue glass bead from an Iron Age site Shisanhang in northern Taiwan (Tsang and Liu 2001). The Guishan sample contains more Na$_2$O but lower CaO than the Shisanhang sample (Na$_2$O ~ 15 wt%, CaO ~ 8 wt%) and thus is different from the Shisanhang sample.

4. Discussion

4.1. Glass bead exchange between Southeast Asia

4.1.1. m-Na-Al Glass

Glass beads at Guishan were recovered from burials of the 3rd to 9th centuries CE. This research has shown that the glass beads are monochrome, mainly drawn or wound, with a m-Na-Al or v-Na-Ca glass composition. M-Na-Al glass compositions dominate at Guishan. This research confirms that this m-Na-Al glass belongs to the sub-type 1, which is the most widespread chemical group of m-Na-Al glass in Southeast Asia in the 1st millennium CE, with an origin which can be linked to Sri Lanka or South India (Dussubieux et al. 2010). As there is no evidence of South Asian contact in Iron Age Taiwan (Wang and Jackson 2014), the dominance of m-Na-Al 1 sub-group confirms the participation of Guishan in the bead exchange network around the South China Sea in the 3rd to 9th centuries. The distribution of bead colours (red, orange, yellow, green and blue) also matches that reported by Dussubieux and her colleagues (Dussubieux et al. 2010).

The orange-red glass beads analysed here from Guishan have parallels with several sites in mainland Southeast Asia, some of which are earlier than Guishan, such as Phum Snay (Cambodia, 350 BCE-200 CE) (Carter, 2013, p. 307), Angkor Borei (Cambodia, 200 BCE-200 CE), others which are later than Guishan, such as Kuala Selinsing (Malaysia, 9th–10th century CE), Sumatra (Indonesia, the 9th century CE) (Dussubieux, 2001, p. 157) and also from Ban Bon Noen in Thailand of unconfirmed date (Pilditch, 1992). Its counterparts are also found at sites in Sri Lanka and South India (Dussubieux, p. 157, 2001; Dussubieux and Gratuze, 2013). In Iron Age Taiwan, orange-red beads are also observed at Shisanhang in northern Taiwan (2nd to 15th centuries CE). The chemical composition of the orange-red beads from Shisanhang have not been analysed, but their counterparts from Southeast Asia and South Asia have an m-Na-Al glass composition, with high barium and low uranium, and so are also characteristic of this m-Na-Al 1 sub-group (Carter, 2013; Dussubieux, 2001), although orange glass from South Asia seems to contain more CaO, K$_2$O, P$_2$O$_5$, MgO and FeO (Dussubieux and Gratuze, 2013, p. 403).

Gratuze (2013) analysed the orange-red glass beads from Cambodia and suggests that the inner red glass and outer orange glass may be two different glass layers, like the production method seen in the Guishan sample. Pilditch (1992) indicates that it is more economical to produce the orange-red layered glass bead than an entirely orange glass bead, and this further suggests these orange glass beads may be inexpensive to produce. Although the workshop(s) of this particular type of glass beads is unknown, its presence at Guishan in the 3rd-9th century CE, as well as at Shisanhang in northern Taiwan, demonstrates the distribution of this orange-red glass from South Asia through Southeast Asia to Taiwan, and also indicates its continuous circulation around the South China Sea region from the late 1st millennium BC to 1st millennium CE.

This research indicates that copper-based ingredients are the most common colouring agents used in the m-Na-Al sub-type 1 glass at Guishan. This is also seen in m-Na-Al sub-type 1 glass from other sites in Iron Age Taiwan (Wang, 2016) as well as in Southeast Asia (Dussubieux, 2001; Dussubieux et al., 2010). The red and orange colour is attributed to reduced cuprous copper, while the blue colour to oxidised cupric copper. It has been reported that the red and orange m-Na-Al sub-type 1 glass show enrichment of FeO, MgO and CaO, which suggest that FeO was deliberately added to facilitate the reduction of copper oxide, and MgO and CaO may be introduced with the Fe-bearing materials

(Dussubieux et al., 2010). Interestingly, in the Guishan samples, increasing amounts of MgO and FeO, but not CaO, are seen in the orange and some red glass samples, and a linear correlation between MgO and FeO can be observed. In these cases, FeO may be intentionally used, as suggested by Dussubieux et al. (2010). This linear correlation is also noted in the blue glass, but not in a few red samples which do not show enrichment of FeO (FeO < 1 wt%) (Fig. 9). Generally, the chemical composition related to the colouring raw materials seems to be less consistent in the red glass than the blue glass, and thus might not point to a single production origin. Taken together the varied minor and trace elemental pattern in the red and blue glass, and the microstructure showing sulphur-containing copper in the red glass but not in the blue glass, may suggest that different copper-bearing raw materials, or recipes, were used in the production of red and blue glass of a m-Na-Al chemical composition. Currently the production of m-Na-Al sub-type 1 glass is associated more with South Asia than Southeast Asia; the results of the Guishan samples possibly reveal a more dynamic exchange network spreading over the Indian Ocean and the South China Sea where the glass production recipe, in particular the use of colourants, is diverse and where the re-distribution of glass objects can be expected in Southeast Asia.

4.1.2. v-Na-Ca glass

V-Na-Ca glass was found in Southeast Asia in increasing amounts from the 7th century CE onwards; its presence is associated with Western Asia (Lankton and Dussubieux, 2006, 2013). The origin of v-Na-Ca glass earlier than 7th century remains less clear, although considering the glassmaking tradition, a Western Asian import is more likely (Lankton and Dussubieux, 2006). In the mid-1st millennium CE in Taiwan, no direct interaction with Western Asian cultures was seen from artefactual evidence. The archaeological records here do not suggest development of any glassmaking either. Therefore the v-Na-Ca glass from Guishan is likely to be acquired through Southeast Asia, originating from Western Asia. The Guishan samples possibly reveal an earlier type of v-Na-Ca glass circulated around the South China Sea region in the mid-1st millennium CE.

Prior to 7th century CE, there are a few v-Na-Ca glasses found in Southeast Asia, including a few objects from sites earlier than Guishan, dated to late 1st millennium BC – 2nd century CE, from Phum Snay (n = 1) and Angkor Borei (n = 4) in Cambodia (Carter, 2013; Dussubieux, 2001), and Khuan Luk Pat (n = 2) in Thailand (Brill, 1999). The majority are dark blue glass. Glass beads of a v-Na-Ca glass composition contemporary to the Guishan samples are limited in Southeast Asia. As yet, only two samples from Prei Khmeng in Cambodia (1st-6th centuries CE) (Carter, 2013) are of overlapped chronology, and these are a dark blue bead and a red–black bead.

Within Taiwan, Guishan currently has the earliest v-Na-Ca glass in association with direct dating to the context where the beads were excavated. Glass samples from other sites in Taiwan, such as Shisanhang and Kiwulan, only have a broad overall site date. A long occupation period was suggested at Shisanhang from the 2nd-15th centuries CE, with intense human activities during 5th-10th centuries (Tsang and Liu, 2001). The similar MgO-K$_2$O grouping of a few v-Na-Ca glasses in the Guishan and Shisanhang (northern Taiwan) samples might suggest the presence of early v-Na-Ca glass at Shisanhang, but a refined chronological scale at Shisanhang, which is not yet available, will help test the possibility. Whilst at Kiwulan, the chronology of glass beads is later than Guishan, dated to 7-12th centuries CE (Chen et al., 2008). A temporal effect may be an explanation for the different MgO-K$_2$O pattern between Guishan and Kiwulan. It is noticed this temporal variation is not only seen in samples from Taiwan, but also in those from Southeast Asia, and thus may reveal a general diffusion across time and space in the range of v-Na-Ca glass compositions around the South China Sea region throughout 1st millennium CE.

For the dark blue glass, the possibility of different sources of cobalt colourant can be observed from the associated elements. Negligible

amounts of As and Zn are observed in Guishan samples (Zn < 40 ppm, As < 15 ppm) as well as the early dark blue glass beads from Angkor Borei and Prei Khmeng in Cambodia (Carter, 2013; Dussubieux, 2001). The later materials exhibit elevated level of Zn, as seen in Sungai Mas in peninsular Malaysia (>3000 ppm), or greater As, as seen in samples from Pulau Kampai in Sumatra (450–915 ppm) (Dussubieux and Allen, 2014; Dussubieux and Soedewo, 2018).

Taken together, the elemental pattern discussed above shows a general similarity between Guishan and early v-Na-Ca glass from Southeast Asia, in particular glass from Cambodia. This does not necessarily suggest that the Guishan samples were imported from Cambodia, as currently the comparative database of early v-Na-Ca glass around the South China Sea is too small to reach a solid conclusion. Alternatively, this possibly indicates that these early v-Na-Ca glass may have been produced using different recipes of plant ash (and perhaps sand with varied impurities or ratios of trace elements), and/or they were coloured by a different source of cobalt to later materials, and furthermore may suggest these are an earlier set of cobalt blue v-Na-Ca glass beads deriving from the South China Sea region, although the production location has yet to be determined.

4.2. Glass bead circulation within Taiwan

It is mentioned above that the Guishan style pottery may reflect the exchange network along the southeastern and the coastal eastern Taiwan. Currently, comparable data for glass beads in this broad area is restricted to a few sites, but a tentative comparison to the beadmaking site at Jiuxianglan (2nd century BCE – 8th century CE) (Wang et al., 2019) and the Blihun Hanben site (ca. late 1st-millennium CE, Chu, 2017) (unpublished analytical data by the author) suggests the circulation of glass beads over the southern part of Taiwan and eastern Taiwan has not intensified.

At Jiuxianglan where there is evidence for glass beadmaking, the bead colour also shows the same balanced distribution as seen at Guishan. All glass beads from Jiuxianglan are drawn beads of a m-Na-Al sub-type 1 glass, but some glass waste is v-Na-Ca glass and indicates a wound method rather than drawn was used. Comparisons in terms of glass chemistry have been made on samples between the two sites, which shows the glass bead exchange is not evident, except for the yellow glass containing bone ash (GS-Y2 group).

A comparison of the v-Na-Ca glass *waste* at Jiuxianglan to the *beads* at Guishan does not suggest they are similar. Higher MgO is found in Jiuxianglan samples (>4 wt%) than Guishan samples (2–4 wt%). It can also be seen in Fig. 10 that the dark blue glass waste from Jiuxianglan displays particularly high Ce (>40 ppm) than the Guishan dark blue beads (<15 ppm). Greater Zn content (1160 ppm) is also found in the dark blue glass waste from Jiuxianglan (Wang et al., 2019). Generally, the glass waste from Jiuxianglan reveals broad similarity to the late v-Na-Ca glass around the South China Sea region. These distinct chemical variations eliminate the possibility that the v-Na-Ca glass beads from Guishan were locally produced at Jiuxianglan. In addition, this may further demonstrate the observation made by Wang et al. (2019) that glass beadmaking may have been taken place at Jiuxianglan no earlier than late 1st millennium CE.

The minor and trace elements in the m-Na-Al glass (all finished beads) from Guishan and Jiuxianglan also reveal differences related to the use of colourants, in particular the green and yellow glass (GS-Y1 group). In the green glass, most Guishan samples have lower Ba (<0.15 wt%) and Sr (<500 ppm) than Jiuxainglan samples (Ba > 0.15 wt% and Sr > 500 ppm). Ba and Sr are generally thought to be introduced with the Ca (Freestone et al. 2003). However, in the case of the Jiuxianglan samples, the elevated concentration of Sr and Ba in the green samples are more associated with the Pb-containing colourant (lead tin oxide) (Wang et al., 2019). The difference of Ba and Sr contents between Guishan and Jiuxianglan samples therefore may result from varied colouring raw materials, which suggests that the green bead samples

from Guishan and Jiuxianglan may not be from the same source. For the yellow glass (GS-Y1 group), various PbO/SnO_2 ratios can be observed in the Guishan and Jiuxianglan samples – the Guishan samples have a ratio consistently smaller than 8 and Jiuxianglan specimens between 10 and 45. At both sites, the yellow colourant is lead tin oxide. The PbO/SnO_2 ratio indicates that different proportions or recipes of lead- and tin-containing ingredients were used in the yellow glass from Guishan and Jiuxianglan.

Despite the variation in chemical compositions seen between Guishan and Jiuxianglan glass beads, it is worthy of pointing out that the yellow glass containing bone ash (GS-Y2 group) found at Guishan is also seen in a glass beadmaking *waste* from Jiuxianglan in southeastern Taiwan (Wang, 2016) and in a yellow glass bead fragment from Blihun Hanben in northeastern Taiwan (unpublished data by the author). In the sample from Jiuxianglan, cubic lead tin oxide is also found within the bone ash, although the concentration of Al_2O_3 and SiO_2 in the bone ash is not as high as those observed in the Guishan samples. In the sample from Blihun Hanben, the bone ash contains a similar content of PbO, Al_2O_3 and SiO_2 to those in Guishan samples, but unfortunately currently there is no minor and trace elemental data of the Blihun Hanben sample that allows further comparison to the Guishan samples. The presence of sodium aluminosilicate and ferromagnesian silicate minerals is found in the sample from Blihun Hanben, supporting the inference that aluminosilicate might have been added into the bone ash.

Jiuxianglan is a beadmaking site, while Blihum Hanben only shows glass bead exchange. The chronology of Jiuxianglan and Blihun Hanben overlaps with the occupation of Guishan and so they are contemporary. As noted above, cultural affinities and object exchange (particular Guishan style pottery) between Guishan (Guishan Culture) and Jiuxianglan (Sanhe Culture) have been suggested by archaeologists in Taiwan. At Blihun Hanben, although Guishan style pottery is also found here, the archaeological assemblage suggests exchange activities along broad eastern Taiwan rather than the cultural affinities as seen between the Guishan Culture and Sanhe Culture. Additionally, the distribution of bead colours at Jiuxianglan are similar to those at Guishan, while at Hanben, our preliminary observation suggests the dominance of orange, yellow and blue glass beads. The yellow glass waste at Jiuxianglan probably provides evidence of the site as a potential beadmaking site using bone-ash containing glass, but the lack of finished objects at Jiuxianglan and the slightly different chemical composition of bone ash glass in the yellow waste from the site make it less conclusive that the beads from here were travelling to Guishan or Blihun Hanben. Nevertheless, the identification of the use of bone ash in all these contemporary beads may suggest the circulation of this type of yellow glass in the far south and in the broad eastern part of Taiwan in the mid- to late-1st millennium, which seems to overlap with the exchange network of Guishan style pottery.

The production centre of this bone ash-containing glass remains obscure. Bone ash acts as opacifier in ancient glass (Turner and Rooksby, 1959). Its presence is reported mostly in natron glass or potash lime silica glass from the eastern part of the Mediterranean Sea and northern Italy before early 1st millennium CE (Towle and Henderson, 2007; Marii and Rehren, 2009; Neri et al., 2017). Previous research reporting bone ash in high alumina glass from around the Indo-Pacific region is found in two white glasses from Sri Lanka, dated to 300 BCE – 900 CE (Welter et al., 2007), but the Al_2O_3 content is lower in the Sri Lankan glass (<5 wt%) than in samples from Taiwan (~8–10 wt%). The Sri Lankan samples also show greater CaO (7.5 wt%) compared to the Taiwanese ones (<2 wt%). It is thus not possible at the current time to suggest any technical connection between the use of bone ash seen in the Taiwanese and Sri Lankan cases, but it is worthy of future attention to inform routes or connections for the possible circulation of this type of glass in the Indo-Pacific region.

Overall, the research suggests that the glass beads found at Guishan are principally foreign imports. The makeup of glass bead colours and the elemental variation in most glass beads implies that glass beads from

Guishan, Jiuxianglan, and possibly Hanben, may not be of a solely overseas origin. The large-scale re-distribution of glass beads is not obvious along the southern end and eastern coastal Taiwan, but small scale glass exchange cannot be eliminated. This is supported by the presence of the bone ash-containing yellow glass at the three sites where there is also circulation of Guishan style pottery. This therefore reveals a more complex exchange network in these wide regions, involving long-distance exchange of exotic beads from various overseas partners to local societies and where the domestic interaction network built upon pottery circulation shows small scale *re-distribution* of these exotic glass beads, or possibly local beadmaking, although at present there is no archaeological evidence for this. The mechanisms which drive this re-distribution are to be elucidated.

5. Conclusion

The excavations at Guishan have yielded 123 monochrome glass beads from 3 burials, dated to 3rd to 9th centuries CE. This research analysed the style, chemical composition and microstructure of 64 glass beads, demonstrating that m-Na-Al glass and v-Na-Ca are the major chemical compositions of the beads at the site and most glass beads were drawn or wound. The m-Na-Al glass comprises >80 percent of the analysed samples and belongs to the m-Na-Al sub-type 1 glass. The chemical composition of the red, orange-red, yellow, green and blue drawn beads is generally consistent with current published findings of this glass composition in Southeast Asia. This evidences the participation of Guishan in the bead exchange network of the South China Sea. Here copper-based colourants are the most commonly used amongst the Guishan samples, and the minor and trace elements and the microstructure of copper-containing crystals possibly show multiple types/recipes of the raw materials used as colouring agents. This suggest the re-distribution of glass beads around the South China Sea region, with a possible origin of the beads in South Asia.

The v-Na-Ca glass, or plant ash glass, at Guishan illustrates the early presence of Western Asian v-Na-Ca glass in the South China Sea exchange network, and its far reach to the far south of Taiwan in mid-1st millennium. That the chemical composition of v-Na-Ca glass at Guishan does not currently fit identified sub-types in late-1st millennium suggests the Guishan samples may represent an earlier type of v-Na-Ca glass circulating in the South China Sea area. This research therefore starts to fill-in the gap for the presence of early v-Na-Ca glass in the wider Southeast Asia.

This study has shown that most Guishan samples are likely to be acquired directly from overseas rather than from the local exchange network along the southern end and broad eastern Taiwan, in particular the glass beadmaking site Jiuxianglan. However, the possibility of local beadmaking, or circulation, of a few glass beads in yellow glass containing bone ash might be suggested.

The scientific investigation of glass beads from Guishan has shown the complexity of the circulation of glass objects between Taiwan and Southeast Asia, indirectly from South Asia and Western Asia. Obviously, the role of Guishan is as the recipient of these exotic glass beads within this wider network. Although the workshops and exact exchange routes remains presently unclear, this research has demonstrated the presence of various scales of exchange behaviours within and between the overseas and domestic networks in a society which is a consumer of glass beads, amongst other material goods. This research fills one more gap in the currently vibrant field of glass bead research around the Indo-Pacific region, which is starting to show an increasingly and ever-changing complex network of glass exchange and production in the region.

CRediT authorship contribution statement

Kuan-Wen Wang: Conceptualization, Methodology, Software, Validation, Investigation, Data curation, Writing - original draft, Writing - review & editing, Visualization, Project administration. **Kuang-Ti Li:**

Appendix A. Supplementary data

Supplementary data to this article can be found online at https://doi.org/10.1016/j.jasrep.2020.102737.

References

Beerkens, R., 1999. Redox and sulphur reactions in glass melting processes. Ceram.-Silikáty 43, 123–131.

Brill, R.H., 1999. Chemical Analyses of Early Glasses, 2. The Corning Museum of Glass, New York.

Carter, A.K., 2013. Trade, Exchange, and Sociopolitical Development in Iron Age (500 BC - AD 500) Mainland Southeast Asia: An Examination of Stone and Glass Beads from Cambodia and Thailand. University of Wisconsin-Madison, Dep. Anthropol.

Chao, C.-Y., Liu, Y.-C., Chung, K.-F., 2013. On 'Upper Huakangshan Culture': a proposal. Field Archaeology of Taiwan 16 (2), 53–79.

Chen, H.-I., 2017. Archaeological Taiwan. Rhythms Monthly, Taipei.

Chen, Y.-B., Chiu, S., Li, C.-Y., 2008. The Rescue Excavation at Kiwulan Site, 1. Lanyang Museum, Yilan.

Chu, C.-Y., 1990. Carbon-14 data in Taiwan. F. Archaeol. Taiwan 1, 95–122.

Chu, C.-Y., 2017. Blihun Hanben Recovered, Reconstructed, Reappeared: Featured Exhibition on Archaeological Excavation Current Result /Exhibition Album. Lanyang Museum, Yilang, Taiwan.

Dussubieux, L., 2014. Compositional analysis of ancient glass fragments from Si Pamutung, North Sumatra. In: Perret, D. (Ed.), History of Padang Lawas, North Sumatra. Association Archipel, Paris, pp. 379–389.

Dussubieux, L., 2001. L'apport de l'blation laser couplée à l'ICP-MS à la caractérisation des verres : application à l'étude du verre archéologique de l'Océan Indien. Université d'Orléans.

Dussubieux, L., Allen, J., 2014. Chemical compositions of glass artifacts from Malaysia: New data from the sites of Kampung Pengkalan Bujang and Sungai Mas. In: Perret, D., Jaafar, Z. b. (Eds.), Ancient Glassware in Malaysia: The Pengkalan Bujang Collection. Department of Museums Malaysia, Kuala Lumpur, pp. 119–161.

Dussubieux, L., Gratuze, B., 2013. Glass in South Asia. In: Janssens, K. (Ed.), Modern Methods for Analysing Archaeological and Historical Glass. vol. 2. John Wiley & Sons, Ltd, New York, pp. 399–413.

Dussubieux, L., Gratuze, B., Blet-Lemarquand, M., 2010. Mineral soda alumina glass: occurrence and meaning. J. Archaeol. Sci. 37, 1646–1655.

Dussubieux, L., Robertshaw, P., Glascock, M.D., 2009. LA-ICP-MS analysis of African glass beads: laboratory inter-comparison with an emphasis on the impact of corrosion on data interpretation. Int. J. Mass Spectrom. 284, 152–161.

Dussubieux, L., Soedewo, E., 2018. The glass beads of Kampai Island, Sumatra. Archaeol. Anthropol. Sci. 10, 1129–1139.

Francis, P., 2002. Asia's Maritime Bead Trade: 300 B.C. to the Present. University of Hawai'i Press, Honolulu.

Freestone, I.C., Leslie, K.A., Thirlwall, M., Gorin-Rosen, Y., 2003. Strontium isotopes in the investigation of early glass production: Byzantine and early Islamic glass from the Near East. Archaeometry 45 (1), 19–32.

Gratuze, B., 1999. Obsidian characterization by Laser Ablation ICP-MS and its application to prehistoric trade in the Mediterranean and the Near East: sources and distribution of obsidian within the Aegean and Anatolia. J. Archaeol. Sci. 26, 869–881.

Gratuze, B., 2013. Glass characterisation using Laser Ablation Inductively Coupled Plasma Mass Spectrometry methods. In: Janssens, K. (Ed.), Modern Methods for Analysing Archaeological and Historical Glass, Modern Methods for Analysing Archaeological and Historical Glass. John Wiley & Sons, Ltd, New York, pp. 201–234.

Huang, S.-C., Chen, Y.-B., Yen, H.-C., 1987. Report of Archaeological and Ethnographic Investigations in the Kenting National Park. Kenting National Park Headquarters, Construction and Planning Administration, Ministry of the Interior, Taiwan (in Chinese).

Hung, H.-C., Bellwood, P., 2010. Movement of raw materials and manufactured goods across the South China Sea after 500 BCE: from Taiwan to Thailand, and back. In: Bellina, B., Bacus, E.A., Pryce, T.O., Christie, J.W. (Eds.), 50 Years of Archaeology in Southeast Asia: Essays in Honour of Ian Glover. River Books, Bangkok, pp. 234–245.

Kaneko, S., 1978. The distribution of shell mounds and their composed mollusk species in Taiwan. Osaka Furitsu Ichioka Koto-gakko Kiyo 2, 1–41.

Kuo, S.-C., 2010. The origin of Paiwan culture traits from archaeological evidence. In: Gadu, M. Z. and Lin, H.-M. (Eds.), 2009 International Symposium on Austronesian Studies. National Museum of Prehistory, Taitung, Taiwan, pp. 185–220. (in Chinese).

Lankton, J.W., Dussubieux, L., 2013. Early glass in Southeast Asia. In: Janssens, K. (Ed.), Modern Methods for Analysing Archaeological and Historical Glass. vol. 2. John Wiley & Sons, Ltd, New York, pp. 415–443.

Lankton, J.W., Dussubieux, L., 2006. Early glass in Asian maritime trade: a review and an interpretation of compositional analyses. J. Glass Stud. 48, 121–144.

Lee, K.-H., 2005. The Report of Rescue Excavation at Jiuxianglan in Taitung County. Taitung County Government, Taitung.

Lee, K.-H., 2009. The human figure motif on pottery from Hsiatuoliang Site. Culture Post: National Museum of Prehistory Letters 25, 38–41.

Lee, K.-H., 2015. The Report of Rescue Excavation at Jiuxianglan in Taitung: Pottery from Cultural Layers. Taitung County Government and National Museum of Prehistory, Taitung.

Lee, K.-H., Yeh, M.-C., 2001. The History of Taitung: The Prehistoric Period. Taitung County Government, Taitung.

Lee, K.-H., Yeh, M.-C., 2017. The Lost Civilisation: Track the Development of Prehistory in Taiwan from the Jiuxianglan Site. Taitung County Government, Taitung, Taiwan.

Li, K.-T., 2003. Ceramic remains from Kueishan and discussions relating to the relationship of Formosan aborigines in southern Taiwan. Bull. Natl. Museum Nat. Sci. 16, 79–90.

Li, K.-T., 2001. The significance of perforated human teeth unearthed from Kuei-shan Site, near the southern tip of Taiwan. Bull. Inst. Hist. Philol. Acad. Sin. 72, 699–722.

Li, K.-T., 1995. The Comparative Study of Prehistoric Settlement in Hengchun Peninsula: A Case Study of Kuei-shan Site and Eluanbi II Site. Planning Bureau of National Marine Biology Museum, Kaohsiung.

Li, K.-T., 1994. Coastal Adaption in Southern Taiwan: A Case Study of Kuei-shan Site and Eluanbi II Site. Planning Bureau of National Marine Biology Museum, Kaohsiung.

Li, K.-T., 1993. Reports on Archaeological Investigations of the Site at National Marine Biology Museum and Kuei-shan Site. Planning Bureau of National Marine Biology Museum, Kaohsiung.

Li, K.-T., Cheng, Y.-S., Ling, P.-C., 1985. Report of Archaeological Investigation in the Kenting National Park on the Southern Tip of Taiwan. National Taiwan University, Taipei, Department of Anthropology.

Liu, Y.-C., Chen, C.-N., Yen, T.-Y., 2002. The Study of Context and Distribution Area of Prehistoric Sites in Taitung County: The Southern Part of Taitung Plain and the Orchid Island. Taitung County Government, Taitung.

Lopes, M., Shelby, J.E., 2007. Introduction to Glass Science and Technology. Royal Society of Chemistry.

Marii, F., Rehren, Th., 2009. Archaeological coloured glass cakes and tesserae from the Petra Church. Ann. 17e Congrès l'Association Int. pour l'Histoire du Verre, pp. 295–300.

Miyamoto, N., 1931. The outline of prehistoric site in Taiwan. Shigaku 10, 689–694.

Neri, E., Jackson, M., O'Hea, M., Gregory, T., Blet-Lemarquand, M., Schibille, N., 2017. Analyses of glass tesserae from Kilise Tepe: New insights into an early Byzantine production technology. J. Archaeol. Sci. Rep. 11, 600–612. https://doi.org/10.1016/j.jasrep.2016.12.036.

Pilditch, J.S., 1992. The Glass Beads of Ban Bon Noen, Central Thailand. Asian Perspect. 31, 171–181.

Stuiver, M., Braziunas, T.F., 1993. Sun, ocean, climate and atmospheric $^{14}CO_2$: an evaluation of causal and spectral relationships. The Holocene 3, 289–305. https://doi.org/10.1177/095968369300300401.

Stuiver, M., Reimer, P.J., Bard, E., Beck, J.W., Burr, G.S., Hughen, K.A., Kromer, B., McCormac, G., Van Der Plicht, J., Spurk, M., 1998. INTCAL98 Radiocarbon Age Calibration, 24,000–0 cal BP. Radiocarbon 40, 1041–1083. https://doi.org/10.1017/S0033822200019123.

Stuiver, M., Reimer, P.J., Braziunas, T.F., 1998. High-precision radiocarbon age calibration for terrestrial and marine samples. Radiocarbon 40, 1127–1151. https://doi.org/10.1017/S0033822200019172.

Sung, W.-X., Yin, C.-C., Huang, S.-C., Lien, C.-M., Liu, Y.-C., 1992. Preliminary Evaluation of the Major Prehistoric Sites of Taiwan. Ethnological Sociaty of China, Taipei.

Towle, A., Henderson, J., 2007. The glass bead game: archaeometric evidence for the existence of an Etruscan glass industry. Etruscan Stud. 10, 47–66.

Tsang, C.-H., Chen, C.-Y., Liu, Y.-C., 1994. A general survey of archaeological sites in Tai-Min area (2nd annual report). Ministry of the Interior, Taiwan.

Tsang, C.-H., Liu, Y.-C., 2001. The Rescue Excavation and Preliminary Research of Shihsanhang Site. Shihsanhang Museum of Archaeology, Taipei.

Tsang, C.-H., Yeh, M.-C., 2000. Report of the Archaeological Sites in Taiwan and Southern Fujian: Taitung County. Institute of History and Philology, Academia Sinica, Taipei.

Turner, W.E.S., Rooksby, H.P., 1959. A study of the opalising agents in ancient glasses throughout three thousand four hundred years. Glas. Berichte 32K, 17–28.

Wagner, B., Nowak, A., Bulska, E., Hametner, K., Günther, D., 2012. Critical assessment of the elemental composition of Corning archeological reference glasses by LA-ICP-

MS. Anal. Bioanal. Chem. 402, 1667–1677. https://doi.org/10.1007/s00216-011-5597-8.

Wang, K.-W., 2016. Cultural and Socio-economic Interaction Reflected by Glass Beads in Early Iron Age Taiwan. University of Sheffield.

Wang, K.-W., 2018. Beads in Iron-Age and Early-Modern Taiwan: An introduction. BEADS: J. Soc. Bead Researchers 30, 16–30.

Wang, K.-W., Iizuka, Y., Hsieh, Y.-K., Lee, K.-H., Chen, K.-T., Wang, C.-F., Jackson, C., 2019. The anomaly of glass beads and glass beadmaking waste at Jiuxianglan, Taiwan. Archaeol. Anthropol. Sci. 11 (4), 1391–1405. https://doi.org/10.1007/s12520-017-0593-3.

Wang, K.-W., Jackson, C., 2014. A review of glass compositions around the South China Sea region (the late 1st millennium BC to the 1st millennium AD): placing Iron Age glass beads from Taiwan in context. J. Indo-Pacific Archaeol. 34, 51–60.

Wang, K.-W., Jackson, C., forthcoming. Social and economic interaction reflected by early Iron Age glass beads from selected sites of Taiwan. In: Muyard, F. and Liu, Y.-C. (Eds.), Maritime Exchange and Localization across the South China Sea, 500 BC–AD 500.

Welter, N., Schüssler, U., Kiefer, W., 2007. Characterisation of inorganic pigments in ancient glass beads by means of Raman microspectroscopy, microprobe analysis and X-ray diffractometry. J. Raman Spectrosc. 38, 113–121. https://doi.org/10.1002/jrs.1637.

Yang, H.-C., Lee, K.-H., Chen, W.-S., 2012. The application of petrographic analysis to archaeological research: examples from the artifacts and sherds of Chiu Hsiang Lan site, Taitung, Taiwan. J. Austronesian Stud. 3, 71–88.

Yeh, M.-C., 1993. The findings and inventory survey of Chulu site in Beinain, Taitung: preliminary exploration on Guishan Culture pottery from Chulu. Bulletion of Preparatory Office of the National Museum of Prehistory, Taiwan 3, 75–93.